J Mol Model (2006) 12: 543–550
DOI 10.1007/s00894-005-0043-5

ORIGINAL PAPER

Mario J. F. Calvete · Danilo Dini · Michael Hanack
Juan Carlos Sancho-García · Weizhe Chen · Wei Ji

Synthesis, DFT calculations, linear and nonlinear optical properties of binuclear phthalocyanine gallium chloride

Received: 3 March 2005 / Accepted: 27 June 2005 / Published online: 8 November 2005

Abstract The axially substituted binuclear GaCl/GaCl phthalocyanine **1** with an unsymmetrical pattern of substitution has been prepared and its nonlinear optical (NLO) properties determined. The resulting binuclear complex retains approximately the same transition energies of monomeric $(RO)_8$PcGaCl as far as the linear optical spectrum is concerned, although **1** has a double concentration of central atoms per molecule and an enlarged conjugated ligand. The lack of significant spectral shifts in passing from mononuclear to binuclear complexes has been rationalized theoretically by means of density functional theory calculations. The purpose of the present study is to determine whether binuclearity affects the optical limiting behavior of **1** with respect to monomeric $(RO)_8$PcGaCl in the NLO regime determined by nanosecond laser pulses.

Keywords Phthalocyanine · Binuclear · Density functional theory · Aromaticity · Nonlinear optics

Introduction

Phthalocyanines (Pcs) are complexes with an extended conjugated network of π-electrons. They present in their structure a central cavity large enough to coordinate almost every positively charged atom of the periodic table [1]. This class of compounds is largely used as active material in various technologies [2–8] mostly because of fast blue-green color due to the HOMO/LUMO and HOMO-1/LUMO transitions [9–11], which have energy values in the broad ranges 1.5–2.0 and 2.5–4.0 eV, respectively [12, 13]. In the UV/vis absorption spectra of Pcs these transitions originate the typical Q- and B-bands within the approximate wavelength ranges 650–800 and 300–450 nm, respectively. The occurrence of broad absorption ranges is a consequence of the availability of a great variety of Pcs structures [14, 15] differing in the number, the nature and the position of substituents [16–20], the nature of the central atoms [12], the nature of the axial ligands [21,22], and the number and linkage between Pc-rings [23–25]. The modulation of the spectroscopic features of Pcs can be thus afforded since it is known that the number and the energy of allowed transitions in the UV/vis spectra of Pcs change with their structure through the modification of the molecular symmetry [26–33], the extent of electronic conjugation [23, 34–37] and the state of aggregation [38–41].

In the present paper, we explore the influence of the enlargement of the π-electron system on the linear and nonlinear optical (NLO) properties of a fused axially substituted binuclear Pc [42–44] with GaCl as central moieties (**1**, Fig. 1). The interest for this type of dimeric structure arises from the opportunity of dealing with condensed Pc-based systems that possess intermediate electronic properties in comparison to separated Pc molecules [36, 37, 42, 43, 45–50], and have double the concentration of central atoms and Pc rings per single molecular unit (Fig. 1). These structural features can be particularly appealing if GaCl is present as central unit when the NLO property of optical limiting (OL) is considered [51–54]. We have previously prepared and characterized a similar axially

Dedicated to Professor Dr. Paul von Ragué Schleyer on the occasion of his 75th birthday.

M. J. F. Calvete · D. Dini · M. Hanack (✉)
Institut für Organische Chemie, Universität Tübingen,
Auf der Morgenstelle 18, 72076 Tübingen, Germany
E-mail: hanack@uni-tuebingen.de
Tel.: +49-7071-2972432
Fax: +49-7071-295268

J. C. Sancho-García
Departamento de Química-Física, Universidad de Alicante,
03080 Alicante, Spain

W. Chen · W. Ji
Department of Physics, National University Singapore,
Science Drive 4, 117542 Singapore, Singapore

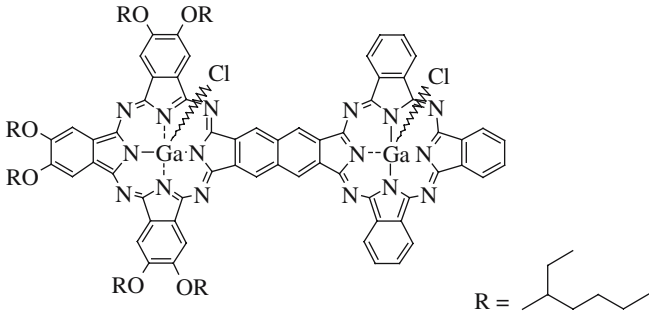

Fig. 1 Structure of binuclear fused GaCl/GaCl phthalocyanine **1**

substituted binuclear Pc with InCl as central moiety [55]. Due to the lack of a significant alteration of the electronic, linear and NLO properties in passing from dimeric side-by-side (InCl)Pc/Pc(InCl) to monomeric PcInCl [55], we decided to focus our attention towards an axially substituted binuclear complex coordinated by a smaller central unit, like GaCl. This is because the distortion of the ligand associated with the coordination of such a smaller central unit is reduced and, consequently, it is expected that the extension of the ligand in binuclear (GaCl)Pc/Pc(GaCl) **1** should lead to more relevant changes in the optical and electronic properties of **1** with respect to the analogous (InCl)Pc/Pc(InCl). The main reason for the choice of an unsymmetrical pattern of substitution with one unsubstituted ring in Pc **1** is due to the relative easiness of separation and purification in the process of synthesis (see Scheme 1).

In order to evaluate the electronic properties of the axially-substituted binuclear fused phthalocyaninato gallium chloride **1**, we have also characterized the extent of its π-delocalization by referring to the harmonic-oscillator model of aromaticity (HOMA) index [56, 57].

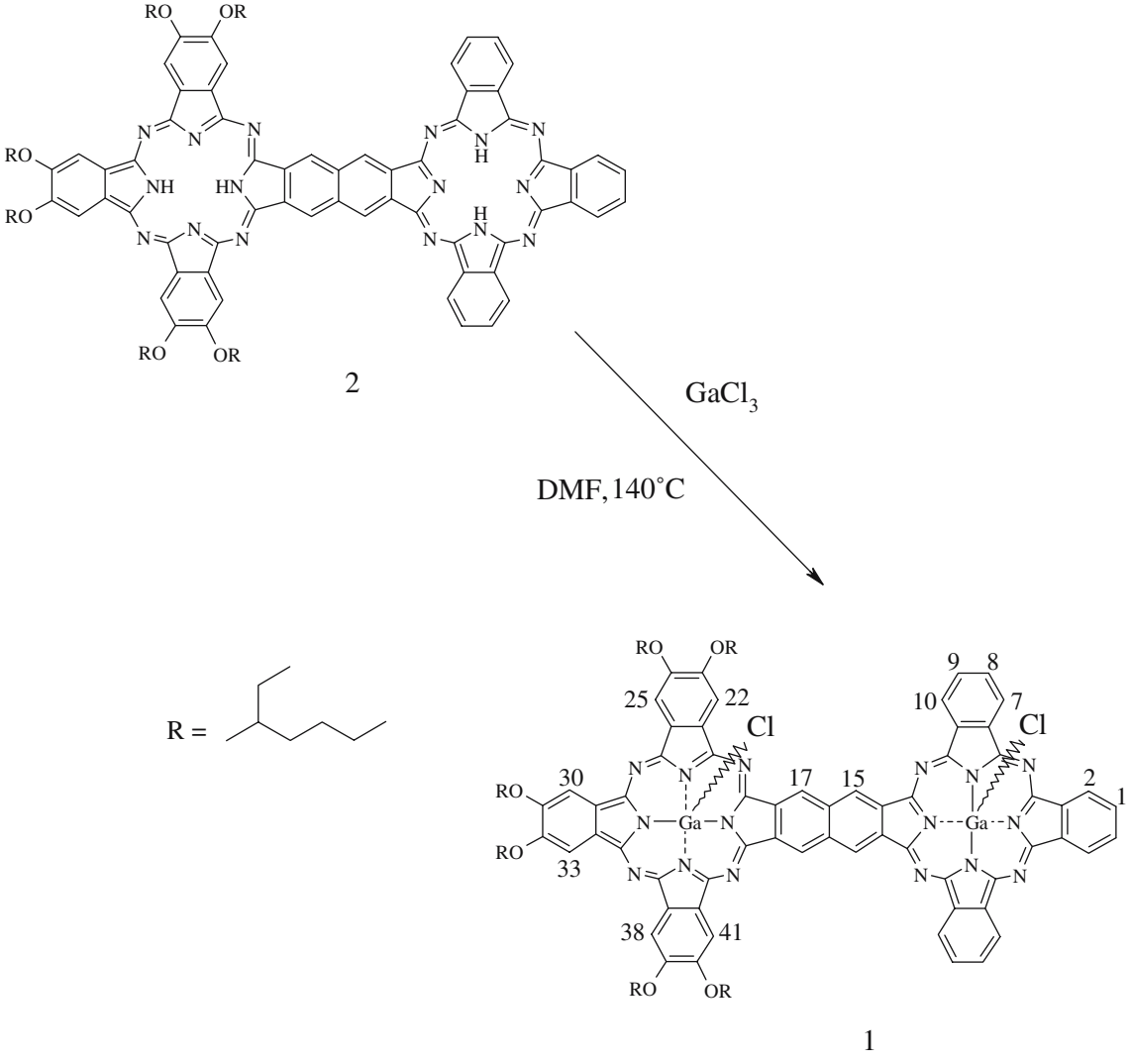

Scheme 1 Synthesis of the binuclear Pc **1**

Experimental part

Synthesis of binuclear GaCl/GaCl Pc 1 (Scheme 1)

Binuclear metal-free Pc **2** [58] (70 mg, 40 μmol) and an excess of $GaCl_3$ (90 mg, 500 μmol) were suspended in DMF. Quinoline (1 ml) was added, the mixture heated till 130°C, and then maintained at this temperature. After completion of the reaction, monitored by UV/vis spectroscopy and thin-layer chromatography for ~5 h, 20 ml of water was added dropwise to the mixture in order to precipitate the compound. After centrifugation, **1** was precipitated three times from hot methanol and dried in vacuum at 100°C. Yield: **1**, 63 mg, (79%), dark green powder. EA**:** Theory, C = 66.84%; H = 6.12%; N = 10.34%; Found: C = 66.02%; H = 5.51%; N = 9.19%. MS (FAB): 1975.7 [M^+], 1,478.2 [M^+-4OR + Na], 1,339.1 [M^+-5OR]. ^{1}H NMR (THF-d_8): δ = 0.90, 1.04, 1.17 1.30 [br, 36H, CH_3], 1.54, [br, 48H, CH_2], 2.04 [br, 6H, CH], 4.25, 4.52 [br, 12H, OCH_2], 6.55 [br, 2H, H-17], 6.68 [br, 2H, H-15], 7.13 [br, s, 6H, H-22, H-25, H-30, H-33, H-38, H-41], 7.92, 7.94 [br, d, 2H, H-2], 8.16, 8.19 [br, d, 2H, H-7], 8.42, 8.45 [br, d, 6H, H-9, H-10], 8.69, 8.71 [br, d, 2H, H-1, H-8]. ^{13}C NMR (THF-d_8): δ = 11.6, 11.9, 12.5, 14.4, 14.8 [CH_3], 23.4, 23.7, 24.1, 26.7, 30.3, 30.6, 31.5, 32.1, 32.9 [CH_2], 40.7, 41.0 [CH], 72.5, 72.7 [OCH_2], 104.2, 105.4, 105.8, 106.6 [C-22, C-25, C-30], 122.0, 123.4, 124.1, [C-1, C-8, C-9], 127.3 [C-15], 128.7 [C-17], 129.9, 130.2, 130.9, [C-2, C-7, C-10], 133.0–137.1 [C-3, C-6, C-11, C-14, C-16, C-18, C-21, C-26, C-29], 140.0–150.7 [C-4, C-5, C-12, C-13, C-19, C-20, C-27, C-28], 153.9, 154.6, 155.6 [C-23, C-24, C- 31]. IR (KBr): ν (cm^{-1}): 2,958, 2,927, 2,859, 1,602, 1,495, 1,457, 1,383, 1,276, 1,201, 1,098, 1,048, 892, 857, 740.7, 565. UV/vis (CH_2Cl_2): λ_{max} = 718.5, 687.5, 654.5, 344.0 nm.

Computational methods

The theoretical evaluation of aromaticity in the axially substituted binuclear Pc **1** used an approach that makes use of the HOMA index [56, 57]. The HOMA index approach is characterized by the evaluation of two main components, EN and GEO, which represent the energetic and geometric contributions of the extent of dearomatization, respectively [57]. The EN term describes changes in aromatic character due to deviation of the average bond length (R_{av}) from an optimal value (R_{opt}), while the GEO term reflects the consequences of bond length alternation. The index was naturally derived, by fixing the empirical value for the constant α (257.7), to give HOMA = 0 for the hypothetical Kekulé structures of aromatic systems and 1 for the system with all bond lengths equal to R_{opt}:

$$\mathrm{HOMA} = 1 - \left[\alpha\left(R_{opt} - R_{av}\right)^2 + \frac{\alpha}{m}\sum_i \left(R_{av} - R_i\right)^2\right] = 1 - \mathrm{EN} - \mathrm{GEO}, \quad (1)$$

where R_i is the length of the ith bond between nonhydrogen atoms out of the m involved in the summation. Equation 1 has also been extended to hetero-π-electron systems, using the Pauling concept of bond number to average properly the parameters involving the heteroatoms [59]. The HOMA index has become one of the most effective ways to quantify the degree of π-delocalization [60–62] over a conjugated fragment. We calculate here the molecular geometries by means of density functional theory (DFT) methods [63–65]. The geometries of compound **1**, either with the chlorine atoms in *syn* or in *anti*, and its corresponding monomer were fully optimized with the B1PW91 exchange-correlation functional, which combines the Becke exchange [66] with the PW91 correlation functional [67] in a hybrid fashion [68]. This methodology is expected to describe the delocalization of the π-electronic cloud in a reliable way while keeping an affordable computational time [69]. A larger portion of exact Hartree-Fock exchange is excluded since the molecular geometries then progressively deteriorate [70]. The cost-effective 6-31G* basis set was accordingly used owing to its good balance between accuracy and computational resources. In the calculations, the oxoalkyl substituents were all replaced by hydrogen atoms since this exchange does not significantly affect the electronic and optical properties of the resulting unsubstituted dimer. On the other hand, this exchange significantly reduces the computational cost. All calculations were performed with the Gaussian 98 program package [71].

The differences between the HOMA values for dimeric metal-free Pc **2** and the dimeric metal complexes (GaCl)Pc/Pc(GaCl) (**1**) and (Mg)Pc/Pc(Mg) (**3**) (**3** has the same structure as **1**, but with Mg as central metal in both rings) [58] are expected to be rather small, as evinced from the small range in which the wavelength values of the Q_{0-0} band vary (c.f. Table 1) [72]. Hence, we confined ourselves to the sole theoretical evaluation of the differences in aromaticity between the topoisomers of compound **1** and its corresponding monomer $(RO)_8$PcGaCl, but not to the compared analysis of the aromaticity of **2** (**3**) with the respective metal-free (Mg) complex.

NLO transmission measurement

The light source used for the determination of NLO transmission of binuclear Pc **1** was a pulsed Nd:YAG laser whose second harmonics of emission were used. The incident beam had a Gaussian profile and the pulse duration was in the range 5–10 ns. NLO transmission curves were taken with f/number = 65 using a Gaussian beam as input beam when the sample is located in correspondence of the beam focus. The choice of such slow optics was made on purpose in order to minimize heating effects during the positioning of the sample around the focal plane. Beam waist is about 40 μm in the experiments of NLO transmission determination.

Table 1 Wavelengths of Q and B bands and molar extinction coefficients (ε) for binuclear Pcs **1**–**3**

Compound	Q_{0-1}/nm [log(ε/mol^{-1} cm^{-1} L)]	Q_{0-0}/nm [log(ε/mol^{-1} cm^{-1} L)]	Q_{1-1}/nm [log(ε/mol^{-1} cm^{-1} L)]	B_{0-0}/nm [log(ε/mol^{-1} cm^{-1} L)]	B_{0-1}/nm [log(ε/mol^{-1} cm^{-1} L)]
1	718.5(sh) [4.61]	687.5 [4.85]	654.5[4.65]	–	344.0 [4.85]
2	688.0 [4.28]	673.0 [4.35]	667.0 (sh) [4.27]	–	358.0 [4.45]
3	706.0 (sh) [4.78]	676.0 [4.89]	652.0 (sh) [4.79]	432.5 [4.73]	362.0 [4.90]
$(RO)_8$PcGaCl	–	694.5 [5.24]	625.0(sh) [4.62]	441.0 [4.38]	357.5 [4.96]
$(RO)_8$PcMg	–	679.0 [5.31]	613.0(sh) [4.69]	–	360.0 [5.01]

All the spectra were recorded in CH_2Cl_2 as solvent. (R = 2-ethylhexyl)

The collection of the transmitted beam was performed in the open-aperture configuration with the same optics as for the incident beam.

The time stability of the liquid samples for NLO experiments was checked through the following three procedures: once a day check per 1 week of the linear optical spectrum of the sample; comparison of the OL measurements obtained when pulse repetition rate was 10 Hz and when the sample was irradiated with a single shot; irradiation of the sample solution with laser pulses at a fixed energy with a repetition rate of 10 Hz for 30 min and successive check of the OL properties. Solvent effects on the OL of the sample solution were studied by measuring OL of the pure solvent. Solvents for OL experiments were used without further purification (commercial spectroscopic grade). Calibration of the optical apparatus was conducted using a reference sample of C_{60} as standard. The OL properties of the different samples were characterized under the same conditions of irradiation and compared with those of the standards.

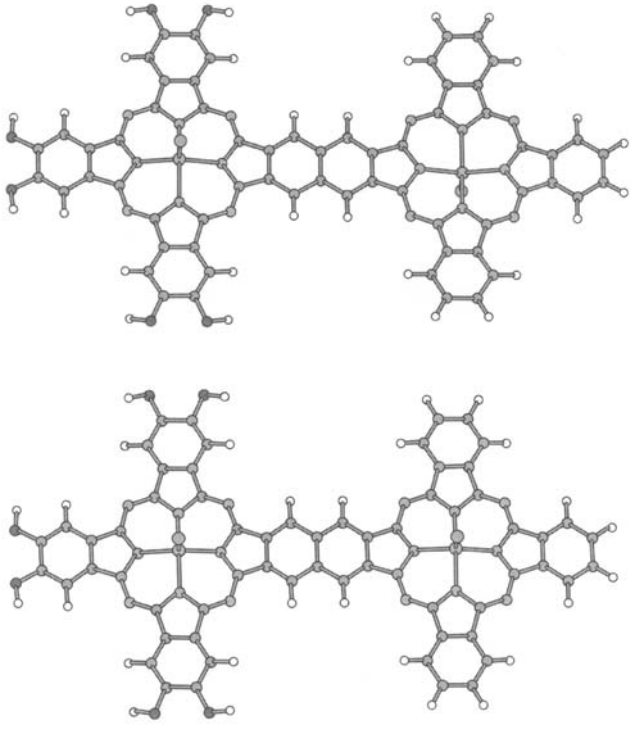

Fig. 2 Density functional theory-optimized structures of the *anti* (*top*) and *syn* (*bottom*) topoisomers of **1**

Results and discussion

The binuclear Pc **2** was prepared by a method recently developed by us [58]. From **2** we could obtain directly the binuclear Pc **1**, containing GaCl, by heating **2** and $GaCl_3$ (in excess) in DMF with a small amount of quinoline at a temperature just below the boiling point of DMF (Scheme 1). Such a procedure represents an extension of the method used for the preparation of dimeric (InCl)Pc/Pc(InCl) by replacing $InCl_3$ with $GaCl_3$ [55].

In the ^{1}H-NMR spectrum of **1**, the aromatic region (range: 6–9 ppm) shows asymmetrical peaks, which are ascribed to aggregation (see experimental). Protons H-25, H-30, H-33 and H-38 are present at 7.13 ppm (Scheme 1), while the signals at 6.55 and 6.68 ppm are attributed to H-17 and H-15, respectively. Protons H-10, H-9 and H-2 appear between 8.45 and 8.71 ppm, while the H-1 and H-8 protons are centered around 8.70 ppm.

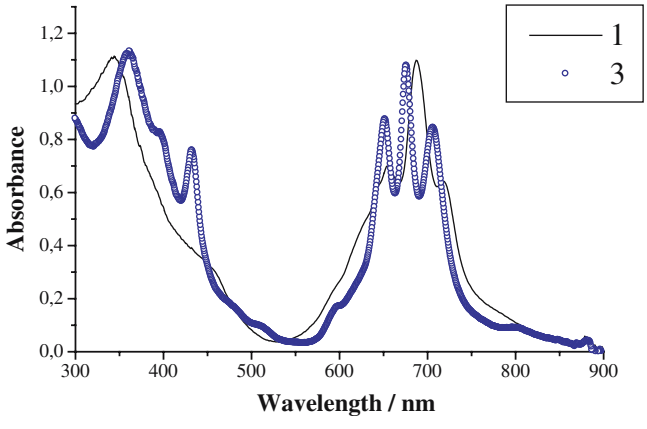

Fig. 3 UV/vis spectra of binuclear (InCl)Pc/Pc(InCl) **1** (*full line*) and (Mg)Pc/Pc(Mg) **3** (*open circles*) (cuvette thickness: 10 mm; concentrations $< 1\times10^{-4}$ M in CH_2Cl_2)

The ^{13}C-NMR spectrum of **1** shows the aromatic carbon peaks for C-22, C-25 and C-30 in the region around 105 ppm. The C-1, C-8, C-9 and C-2, C-7, C-10 carbon atoms of the unsubstituted part of the binuclear Pc are assigned around 123 and 130 ppm, respectively. Carbons C-15 and C-17 are located at 127.3 and 128.7, respectively. The alkyloxy substituted aromatic carbons C-23, C-24, C-31 are observed at about 155 ppm.

The IR spectrum of **1** resembles that of mononuclear Pcs, but the IR spectrum of **2** (metal-free binuclear Pc) shows the typical NH-stretching band at 3,298 cm^{-1} whereas **1** does not show such a band because of metalation.

From the analysis of the reported spectra we could not decide whether **1** is constituted by one isomer (with chlorines either in *syn* or *anti*), or a mixture of both forms [49]. The ordinary techniques would not allow the separation of the different topoisomers of **1**, as shown earlier with similar compounds [73].

From DFT-calculations, the *anti* conformation of **1** is predicted to be 6.35×10^{-23} J (=0.16 kcal mol^{-1}) more stable in the gas phase than the *syn* form. It must be noted that this tiny energy barrier is lower than K_BT at room temperature ($k_BT=4.11\times10^{-21}$ J at $T=298$ K being k_B the Boltzmann's constant). The steric hindrance of the *syn* isomer is the factor determining the relative stability of the two isomers, thus pointing to the existence of a subtle compromise between steric and possible π-delocalization effects in the binuclear complexes. The DFT-optimized structures are shown in Fig. 2. Note that the slight deviation from planarity for the rings of the macrocycle, driven by the presence of a coordinating central atom, might be largely reduced in the solid state due to packing effects.

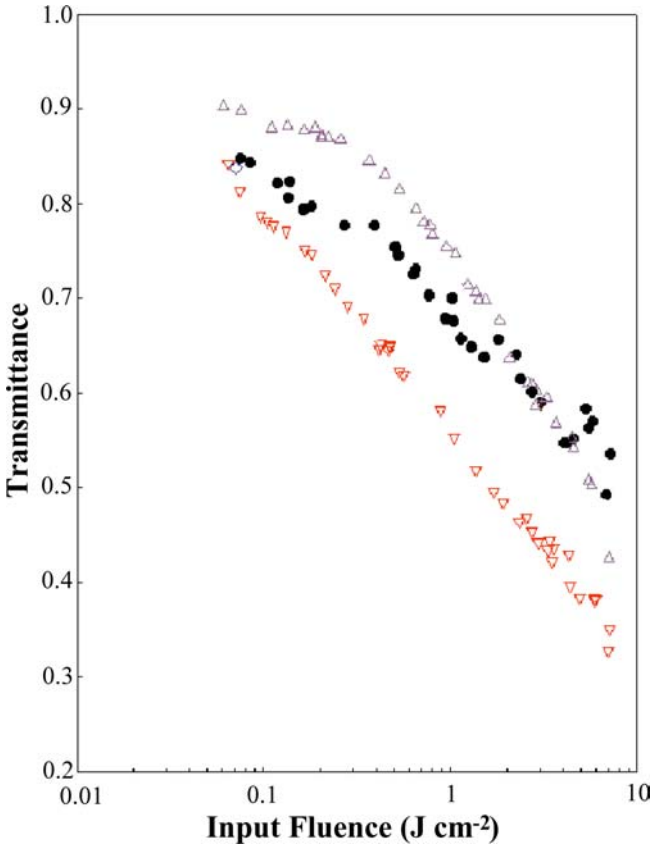

Fig. 4 Nonlinear transmission curves of binuclear Pc **1** (*up triangles*), C_{60} (*black circles*), and monomeric $(RO)_8$PcGaCl [R = 2-ethylhexyl] (*down triangles*) at 532 nm for 7 ns pulsed radiation. Cuvette thickness: 1 mm; concentrations (in g L^{-1}): 0.1, 0.80 in toluene for **1** and $(RO)_8$PcGaCl, respectively. Beam waist at the focus: 40 μm. Concentration of C_{60} solution was chosen in such a way that its linear transmission at 532 nm was $T_0=0.85$

UV/vis spectra of axially substituted binuclear Pc 1

The UV/vis maxima of binuclear Pcs **1** and **2** (in CH_2Cl_2) are given in Table 1. When comparing the optical spectra of the binuclear Pcs **1** and **3** [58] with the respective monomers $(RO)_8$PcGaCl (R = 2-ethylhexyl) and $(RO)_8$PcMg (R = 2-ethylhexyl) [58], respectively, a very weak blue-shift is observed for the more intense peak of the group of Q-bands of the binuclear systems. In other words, the two condensed Pc rings in **1** have an almost independent behavior in terms of π-electron delocalization. Actually, no mesomeric structures of compound **1** including both rings can be drawn. The shoulder of the Q-band in the UV/vis spectra of **1** (Fig. 3) shows a red-shift of the band of approximately 25 nm in the binuclear systems with respect to the mononuclear counterparts (Table 1). Similar to the trend observed with mononuclear complexes $(RO)_8$PcGaCl and $(RO)_8$PcMg, the binuclear Pcs **1** and **3** (Fig. 1) also exhibit a red-shift in going from binuclear Mg/Mg **3** [58], to the binuclear (GaCl)Pc/Pc(GaCl) **1** (Fig. 3). The observed red-shifted shoulders are mainly due to the influence of the different central metals rather than a more extended delocalization of the conjugated electrons in the binuclear complexes. Similar results were also found by comparing the optical spectrum of monomeric *t*-Bu_4PcInCl [74] with that of binuclear (InCl)Pc/Pc(InCl) [55].

Theoretical evaluation of aromaticity in binuclear Pc 1

The DFT-calculated EN, GEO, and HOMA values for the different isomers of **1** are shown in Table 2. The HOMA index for monomeric $(RO)_8$PcGaCl was also computed and it results to be 0.794 at the B1PW91/6-31G* level. From the analysis of the HOMA indexes of the dimeric isomers and the monomer, it results that the *syn* isomer of **1** has the closest value (0.771) to that of the monomer (0.794) with respect to the *anti* isomer (0.715). Since there is no significant difference between the positions of the Q_{0-0} band of the monomer $(RO)_8$PcGaCl (694.5 nm) and the one of the dimeric compound **1** (687.5 nm) in the experimental UV/vis spectra (Table 1), a larger presence of the *syn* isomer in the actual mixture of isomers is predicted from HOMA index comparison. From calculations it is generally found a decrease in

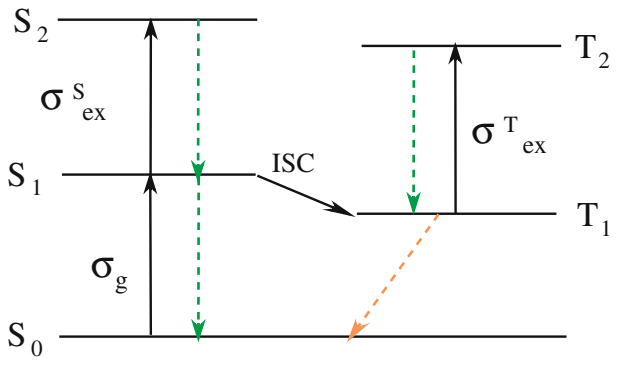

Fig. 5 Jablonski diagram for the description of the mechanism of reverse saturable absorption (*RSA*) upon short-pulse irradiation of cromophores like phthalocyanines, in the visible spectrum. S_0, $S_{1(2)}$ and $T_{1(2)}$ indicate the singlet ground state, the first (second) excited singlet state and the first (second) excited triplet state, respectively. The cromophore absorbs the first photon through the transition $[S_0 \rightarrow S_1]$, and, depending on the dynamics of the irradiated system, will absorb sequentially a second photon through either $[S_1 \rightarrow S_2]$ or $[T_1 \rightarrow T_2]$ transition. $\sigma_{ex}^{S(T)}$ and σ_g are the absorption cross sections from the excited singlet (triplet) state and the ground state, respectively. Verification of RSA implies that $\sigma_{ex}^{S(T)} > \sigma_g$. *Skew* and *straight downward arrows* indicate phosphorescence and fluorescence decays, respectively. ISC is the acronym for intersystem crossing $[S_1 \rightarrow T_1]$. For sake of clarity only the fundamental vibrational level of the various electronic levels is indicated

aromaticity in passing from the monomer to either of the dimeric isomers. This is determined by the relatively large values of the GEO terms, which are related with the bond length alternation. GEO terms result to be about twice the values of the EN terms (Table 2). Such findings imply that the dimer has rings with more localized double bonds and, therefore, is a less aromatic system with respect to the monomer. This is in accordance with the experimental observation of the red-shift of the $Q_{0\text{-}0}$ band in passing from monomeric $(RO)_8$PcGaCl to dimeric (GaCl)Pc/Pc(GaCl) **1** and it is theoretically confirmed by the lower HOMA values of the binuclear dimeric Pc with respect to the mononuclear system. Therefore, both the analyses of the position of the $Q_{0\text{–}0}$ absorption band and the values of HOMA index lead to the same conclusion: dimeric Pc **1** behaves almost like a monomeric Pc in terms of π-delocalization.

Nonlinear optical transmission of binuclear Pc 1

The variation of optical transmission of the axially substituted binuclear (InCl)Pc/Pc(InCl) **1** in toluene at 532 nm is shown in Fig. 4 when the incident radiation is produced by 7 ns laser pulses. For comparison, the profiles of NLO transmission under analogous conditions for mononuclear $(RO)_8$PcGaCl with R = 2-ethylhexyl [58] and C_{60} are also reported. At 532 nm the linear transmission of sample **1** is $T_0 = 0.88$. The limiting threshold T_{lim}, defined as the value of incident fluence at which the NLO transmission T of sample **1** corresponds to $T_0/2$, is 7.6 J cm^{-2}. From the trend in Fig. 4, it is found that **1** behaves as a reverse saturable absorber [75] since its solution in toluene reduces continuously its optical transmission upon increase of the incident fluence within the range 0–10 J cm^{-2}. The wavelength of analysis (532 nm) corresponds approximately to the minimum of linear optical absorption comprised between the enlarged Q and B absorption bands of **1** (Fig. 3). In correspondence of such a minimum of linear optical absorption (which is equivalent to a minimum of the ground-state absorption cross section), it is expected that the OL effect in the nanosecond pulse regime will have an optimum [74–77]. For complex **1**, the occurrence of such an NLO phenomenon at 532 nm is due to a mechanism of sequential two-photon absorption (Fig. 5). In this case an excited electronic state is formed upon absorption of the first photon, and it absorbs at the same wavelength more efficiently than the ground state [74, 76, 77]. For binuclear (GaCl)Pc/Pc(GaCl) phthalocyanine **1**, it has been observed that such an excited state absorbs light pulses with duration of several nanoseconds (pulse duration range: 3–10 ns). This implies that the lifetime of the absorbing excited state cannot be shorter than 10 ns for **1** under the experimental conditions used. If the absorbing excited state is not directly formed upon absorption of the first photon from the ground state, then the internal conversion time τ_{IC}, i.e. the time necessary for the system to be transformed into the most stable level of an excited state, must be shorter than the pulse duration, i.e. $\tau_{IC} < 3\text{–}10$ ns. Upon nanosecond pulses irradiation in Pcs, as intersystem crossing process occurs and the formation of the highly absorbing excited state is accompanied by the change of spin state after absorption of the first photon (Fig. 5) [78].

From the comparison of the OL curve of the binuclear system **1** and mononuclear $(RO)_8$PcGaCl [38] (Fig. 4) it is evident that the monomer has a stronger limiting effect when the linear transmission values are approximately the same. Such a difference is due to the higher tendency of aggregation for the dimer **1** with respect to the monomer $(RO)_8$PcGaCl, since the dimer presents an unsubstituted part, which has a somewhat stronger tendency to aggregate. As a consequence, the generation of the highly absorbing excited state is impeded by the presence of this unsubstituted half and brings about to a generally lower effectiveness of the OL effect for the dimeric complex **1**. As discussed before, an increase of electronic conjugation in dimer **1** with respect to the monomeric species due to the enlargement of the structure, is actually not verified as witnessed by the absence of red-shift in the linear absorption spectrum of **1** when compared to the monomeric counterpart.

Table 2 Density functional theory-calculated EN, GEO, and HOMA values for binuclear Pc **1**

	EN	GEO	HOMA
Syn	0.078	0.151	0.771
Anti	0.104	0.181	0.715

Therefore, it results that the OL effect from dimer **1** is a phenomenon that involves only the electronic excitation of a single Pc ring similarly to what we have previously found in the analysis of the NLO transmission of binuclear (InCl)Pc/Pc(InCl) [55].

Conclusions

The objective of the present work was the synthesis and full characterization of the binuclear axially substituted (GaCl)Pc/Pc(GaCl) **1**. Metal-free binuclear Pc **2** was the starting material for the preparation of binuclear Pc **1** containing GaCl (Scheme 1).

The theoretical evaluation of the extent of electronic delocalization and aromaticity in axially substituted binuclear Pc **1** has been accomplished by means of the harmonic oscillator model of aromaticity index. It is found that the two condensed Pc rings show almost independent behavior in terms of π-electrons delocalization, no mesomeric structures of compound **1** including both rings can be drawn. This is in agreement with the experimental spectral features of the binuclear complexes when compared to the spectrum of the mononuclear species $(RO)_8$PcGaCl. The absence of any electronic delocalization in **1** implies that this dimeric complex is equivalent to a species with a double concentration of Pc ring and central moieties per single molecular unit with no lateral interaction.

The OL effect produced by **1** was determined in the NLO regime determined by nanosecond laser pulses at 532 nm and it confirms the independent behavior of the two Pc rings. **1** behaves as a reverse saturable absorber via the mechanism of sequential two-photon (or excited state) absorption with a limiting threshold 7.6 J cm^{-2}. Binuclear Pc **1** is thus a less effective optical limiter than the monomeric system $(RO)_8$PcGaCl due to a higher tendency of aggregation for the dimer in solution.

Acknowledgements Financial support from EU project "NANOCHANNEL" (Grant No. HPRN-CT-2002-00323) is gratefully acknowledged. The work in Alicante is supported by the "Ministerio de Educacion y Ciencia" of Spain and the "European Regional Development Fund"through project CTQ2004-06519/BQU; the regular grants of the "Vicerrectorado de Investigación" of the University of Alicante (VIGROB2004-36) are also acknowledged.

References

1. Leznoff CC, Lever ABP (eds) (1989–1996) Phthalocyanines: properties and applications, vol 1–4. VCH, Cambridge
2. Hanack M, Lang M (1994) Adv Mat 6:819–833
3. Erk P, Hengelsberg H (2003) In: Kadish KM, Smith KM, Guilard R (eds) The porphyrin handbook, vol 19. Elsevier, Amsterdam, pp 105–150
4. Simon JJ, Andre' HJ (1985) Molecular semiconductors. Springer, Berlin Heidelberg New York
5. Law KY (1993) Chem Rev 93:449–486
6. Dini D, Barthel M, Hanack M (2001) Eur J Org Chem 3759–3769
7. Hurditch R (2001) Adv Colour Sci Techn 4:33–40
8. Gregory P (1991) High technology applications of organic colorants. Plenum, New York
9. Goutermann M (1977) In: Dolphin R (ed) The porphyrins, vol 3. Academic, New York, pp 1–157
10. Stillman MJ, Nyokong T (1989) In: Leznoff CC, Lever AJP (eds) Phthalocyanines: properties and applications, vol 1. VCH, Weinheim, pp 133–257
11. Lever ABP, Pickens SR, Minor PC, Licoccia S, Ramaswamy BS, Magnell K (1981) J Am Chem Soc 103:6800–6806
12. Dini D, Hanack M (2003) In: Kadish KM, Smith KM, Guilard R (eds) The porphyrin handbook, vol 17. Elsevier, Amsterdam, pp 1–36
13. Dini D, Hanack M (2004) J Porphyrins Phthalocyanines 8:915–933
14. Hanack M, Heckmann H, Polley R (1997) In: Schaumann E (ed) Methods of organic chemistry (Houben-Weyle-Hetarenes IV: six-membered and larger hetero-rings with maximum insaturation), vol E9d. Georg Thieme Verlag, Stuttgart, pp 717–842
15. McKeown NB (2004) In: Weinreb SM (ed) Science of synthesis (Houben-Weyle, Methods of molecular transformations-hetarenes and related ring systems), vol 17. Georg Thieme Verlag, Stuttgart, pp 1237–1368
16. Cook MJ (2002) Chem Rec 2:225–236
17. Cook MJ (1994) J Mat Sci 5:117–128
18. Schmid G, Witke E, Schlick U, Knecht S, Hanack M (1995) J Mat Chem 5:855–859
19. Rager C, Schmid G, Hanack M (1999) Chem Eur J 5:280–288
20. Winter G, Heckmann H, Haisch P, Eberhardt W, Hanack M, Lueer L, Egelhaaf HJ, Oelkrug D (1998) J Am Chem Soc 120:11663–11673
21. Barthel M, Hanack M (2000) J Porphyrins Phthalocyanines 4:635–638
22. Chen Y, Subramanian LR, Barthel M, Hanack M (2002) Eur J Inorg Chem 1032–1034
23. Kobayashi N (2002) Coord Chem Rev 227:129–152
24. Cook MJ (1995) Adv Mat 7:877–880
25. Hanack M, Dini D (2003) In: Kadish KM, Smith KM, Guilard R (eds) The porphyrin handbook, vol 18. Elsevier, Amsterdam, pp 215–280
26. Kobayashi N, Nakajima SI, Ogata H, Fukuda T (2004) Chem Eur J 10:6294–6312
27. Kobayashi N, Ogata H (2004) Eur J Inorg Chem 906–914
28. Fukuda T, Ono K, Homma S, Kobayashi N (2003) Chem Lett 32:736–737
29. Kobayashi N, Mack J, Ishii K, Stillman MJ (2002) Inorg Chem 41:5350–5363
30. Kobayashi N, Miwa H, Nemykin V (2002) J Am Chem Soc 124:8007–8020
31. Kobayashi N, Konami H (2001) J Porphyrins Phthalocyanines 5:233–255
32. Kobayashi N, Muranaka A, Ishii K (2000) Inorg Chem 39:2256–2257
33. Nemykin VN, Kobayashi N, Nonomura T, Lukyanets EA (2000) Chem Lett 184–185
34. Orti E, Piqueras MC, Crespo R, Bredas JL (1990) Chem Mat 2:110–116
35. Orti E, Bredas JL, Clarisse C (1990) J Chem Phys 92:1228–1235
36. Kobayashi N, Higashi Y, Osa T (1994) J Chem Soc Chem Commun 1785–1786
37. Kobayashi N, Lam H, Nevin WA, Janda P, Leznoff CC, Koyama T, Monden A, Shirai H (1994) J Am Chem Soc 116:879–890
38. Snow AW (2003) In: Kadish KM, Smith KM, Guilard R (eds) The porphyrin handbook, vol 18. Elsevier, Amsterdam, pp 129–176
39. Monahan AR, Brado JA, De Luca AF (1972) J Phys Chem 76:1994–1996
40. George RD, Snow AW, Shirk JS, Barger WR (1998) J Porphyrins Phthalocyanines 2:1–7
41. Choi MTM, Li PPS, Ng DKP (2000) Tetrahedron 56:3881–3887

42. Calvete M, Hanack M (2003) Eur J Org Chem 2080–2083
43. Leznoff CC, Lam H, Marcuccio SM, Nevin WA, Janda P, Kobayashi N, Lever ABP (1987) J Chem Soc Chem Commun 699–701
44. Yang J, van de Mark MR (1993) Tetrahedron Lett 34:5223–5226
45. Kobayashi N, Higashi Y, Osa T (1991) J Chem Soc Chem Commun 1203–1205
46. Fukuda T, Stork JR, Potucek RJ, Olmstead MM, Noll BC, Kobayashi N, Durfee WS (2002) Angew Chem 114:2677–2680
47. De la Torre G, Martinez-Diaz MV, Torres T (1999) J Porphyrins Phthalocyanines 3:560–568
48. De la Torre G, Martinez-Diaz MV, Ashton PR, Torres T (1998) J Org Chem 63:8888–8893
49. Claessens CG, Torres T (2002) Angew Chem Int Ed 41:2561–2565
50. Ishii K, Kobayashi N, Higashi Y, Osa T, Lelievre D, Simon J, Yamauchi S (1999) Chem Commun 969–970
51. Bertagnolli H, Blau WJ, Chen Y, Dini D, Feth MP, O'Flaherty SM, Hanack M, Krishnan V (2005) J Math Chem 15:683–689
52. Chen Y, Fujitsuka M, O'Flaherty SM, Hanack M, Ito O, Blau WJ (2003) Adv Mat 15:899–902
53. Chen Y, O'Flaherty SM, Fujitsuka M, Hanack M, Subramanian LR, Ito O, Blau WJ (2002) Chem Mat 14:5163–5168
54. Chen Y, Subramanian LR, Fujitsuka M, Ito O, O'Flaherty SM, Blau WJ, Schneider T, Dini D, Hanack M (2002) Chem Eur J 8:4248–4254
55. Calvete MJF, Dini D, Flom SR, Hanack M, Pong RGS, Shirk JS (2005) Eur J Org Chem 3499–3509
56. Kruszewski J, Krygowski TM (1972) Tetrahedron Lett 13: 3839–3842
57. Krygowski TM, Cyrański M (1996) Tetrahedron 52:1713–1722
58. Calvete M (2003) PhD Thesis, University of Tuebingen
59. Krygowski TM, Cyrański M (1996) Tetrahedron 52:10255–10264
60. Krygowski TM, Cyrański M (2001) Chem Rev 101:1385–1419
61. Poater J, Fradera X, Durán M, Solá M (2003) Chem Eur J 9:1113–1122
62. Sancho-García JC, Brédas JL, Beljonne D, Cornil J, Martínez-Álvarez R, Hanack M, Poulsen L, Gierschner J, Mack HG, Egelhaaf HJ, Oelkrug D (2005) J Phys Chem B (to be published)
63. Kohn W, Sham LJ (1965) Phys Rev A 137:1697–1705
64. Lieb E (1983) Int J Quantum Chem 24:243–277
65. Parr RG, Yang W (1989) Density-functional theory of atoms and molecules. Oxford University Press, New York
66. Becke AD (1988) Phys Rev A 38:3098–3100
67. Perdew JP (1991) Electronic structure of solids. Akademie, Berlin
68. Perdew JP, Ernzenhof M, Burke K (1996) J Chem Phys 105:9982–9985
69. Sancho-García JC, Pérez-Jiménez AJ (2004) Recent Res Dev Chem Phys 5:157–171
70. Adamo C, Barone V (1997) Chem Phys Lett 274:242–250
71. Frisch MJ, Trucks GW, Schlegel HB, Scuseria GE, Robb MA, Cheeseman JR, Zakrzewski VG, Montgomery JA, Stratman RE, Burant JC, Dapprich S, Millam JM, Daniels AD, Kudin KN, Strain MC, Farkas O, Tomasi J, Barone V, Cossi M, Cammi R, Mennucci B, Pomelli C, Adamo C, Clifford S, Ochterski J, Petersson GA, Ayala PY, Cui Q, Morokuma K, Malick DK, Rabuck AD, Raghavachari K, Foresman JB, Cioslowski J, Ortiz JV, Baboul AG, Stefanov BB, Liu C, Liashenko A, Piskorz P, Komaromi I, Gomperts R, Martin RL, Fox DJ, Keith T, Al-Laham MA, Peng CY, Nanayakkara A, Gonzalez C, Challacombe M, Gill PMW, Johnson BG, Chen W, Wong MW, Andres JL, Gonzales C, Head-Gordon M, Replogle ES, Pople JA (1998) Gaussian 98. Gaussian Inc, Pittsburgh
72. Cyranski MK, Krygowski TM, Wisiorowski M, Van Eikema Hommes NJR, Von Ragué Schleyer P (1998) Angew Chem Int Ed 37:177–180
73. Hauschel B, Jung R, Hanack M (1999) Eur J Inorg Chem 693–703
74. Shirk JS, Pong RGS, Flom SR, Heckmann H, Hanack M (2000) J Phys Chem A 104:1438–1449
75. Van Stryland EW, Sheik-Bahae M, Said AA, Hagan DJ (1993) Progr Cryst Growth Charact 27:279–311
76. Perry JW, Mansour K, Lee IYS, Wu XL, Bedworth PV, Chen CT, Ng D, Marder SR, Miles P (1996) Science 273:1533–1536
77. Nalwa HS, Shirk JS (1996) In: Leznoff CC, Lever AJP (eds) Phthalocyanines: properties and applications, vol 4. VCH, Weinheim, pp 79–181
78. Turro NJ (1978) Modern molecular photochemistry. Benjamin/Cummings, Menlo Park